EAST-WEST STATION-KEEPING MANOEUVRE

M. Utashima A. Tanaka T. Tohchi T. Ogino

Tsukuba Space Center
National Space Development Agency
Ibaraki, Japan

Fujitsu Limited
Tokyo, Japan

Mitsubishi Electric
Corporation
Kamakura, Japan

ABSTRACT

Because of the presence of small perturbing forces on orbit, the position of an initially geostationary satellite relative to the earth will be disturbed. Therefore, the periodical station-keeping maneuvers are required to maintain the satellite in its station against various perturbing forces. In order to determine an optimum station-keeping maneuver, it is necessary to analyze the perturbed motion of a geostationary satellite and the effect of an impulsive velocity increment on it. NASDA developed an east-west station-keeping maneuver strategy which is called "Sun-synchronized Method". Moreover, a maneuver evaluation technique is also obtained from the analysis of the effect of the impulsive velocity increment on a geostationary satellite.

These techniques have given very satisfactory results in the operations of the station-keeping maneuvers for the existing satellites.

Keywords: East-west Station-keeping, Geostationary Satellite, Perturbation, Mean Element, Impulsive velocity Increment, Maneuver Evaluation, Sun-synchronized Method

1. INTRODUCTION

National Space Development Agency of Japan (NASDA) has launched several geostationary satellites. In order to keep the stations of these satellites, NASDA analyzed the perturbations on the geostationary orbit and the effects of an impulsive velocity increment on it, and then developed the east-west station-keeping maneuver strategy which is called "Sun-synchronized Method" and the maneuver evaluation method.

At first, this paper describes the results of the analyses of the perturbations on a geostationary orbit, and the effect of an impulsive velocity increment on it. Then the Sun-synchronized method and the maneuver evaluation method are described. The final part of this paper presents the results of east-west station-keeping maneuvers, which have been carried out based upon the Sun-synchronized method, for CS(Medium-capacity Communications Satellite for Experimental Purposes).

2. PERTURBATIONS ON GEOSTATIONARY ORBIT

The principal perturbations on a geostationary orbit are due to the triaxiality of the earth, luni-solar gravitational effects, and solar radiation pressure. The triaxiality of geogravitational field and solar radiation pressure tend to induce in-plane perturbations. The ellipticity of the equator causes a long-period variation of the sub-satellite longitude. Solar radiation pressure causes an annual variation of the eccentricity. On the other hand the earth's oblateness and the luni-solar gravitational attractions generate mainly out-of-plane perturbations. These induce long-period variations of inclination and ascending node. The actual motion of geostationary satellite under the influence of all perturbations is a sum of many short-period perturbations with different frequencies, amplitudes, and phases superimposed on the long-period perturbations.

Analyzing the perturbed motion of a geostationary satellite in detail, it becomes possible to attain an exact maneuver strategy. In order to analyze the effect of perturbations on a geostationary orbit, the following orbital elements are used:

- semi-major axis a
- mean right ascension $\Sigma = \Omega+\omega+M$
- inclination vector (i-vector) $\begin{pmatrix} p \\ q \end{pmatrix} = \sin i \begin{pmatrix} \cos \Omega \\ \sin \Omega \end{pmatrix}$
- eccentricity vector (e-vector) $\begin{pmatrix} \xi \\ \eta \end{pmatrix} = e \begin{pmatrix} \cos(\Omega+\omega) \\ \sin(\Omega+\omega) \end{pmatrix}$

where Ω is the right ascension of the ascending node, ω the argument of perigee, M the mean anomaly, i the orbital inclination, and e the eccentricity.

2.1 Short-period perturbations

Obviously, it is impossible to correct periodical perturbations unless their period is much longer than the maneuver cycle. The short-period perturbations must be separated from the osculating elements to determine an optimum maneuver. Given the osculating elements, it is necessary to obtain the corresponding mean elements which omit the effect of the short-period, about 1 day or less, perturbations. In order to obtain the mean elements, it is necessary to know the daily variations of the elements caused by short-period perturbations.

Proc. Int. Symp. Spacecraft Flight Dynamics, Darmstadt, FRG, 18-22 May 1981 (ESA SP-160, Aug. 1381)

For a geostationary orbit, the following three elements are significantly perturbed by the short-period terms: 1) semi-major axis, 2) mean subsatellite longitude defined as $\lambda m = \Sigma - \theta g = \Omega + \omega + M - \theta g$ where θg is the Greenwich sidereal time, and 3) eccentricity vector.

2.1.1 Semi-major axis. Lunar and solar gravitational attractions, and solar radiation pressure cause the changes in the osculating semi-major axis with the amplitudes of about 1Km, 0.5Km, and 0.03Km (for CS) respectively.

2.1.2 Mean subsatellite longitude. Lunar and solar gravitational attractions cause the changes in λm with the amplitudes of about 0.002° and 0.001° respectively.

2.1.3 Eccentricity vector. The second zonal term (J_{20}-term) of earth's potential, and luni-solar gravity cause the changes in eccentricity vector with amplitudes 0.4×10^{-4}, 0.5×10^{-4}, and 0.2×10^{-4} respectively. The daily variations of e-vector due to these perturbing forces are given by the following equations.

For J_{20}-term:

$$\begin{pmatrix} \Delta\xi_J \\ \Delta\eta_J \end{pmatrix} = \frac{3}{2} J_2 \left(\frac{a_e}{a}\right)^2 \begin{pmatrix} \cos \Sigma \\ \sin \Sigma \end{pmatrix} \qquad (1)$$

where a_e is the mean equatorial radius and J_2 is the coefficient for J_{20}-term. This indicates that the e-vector perturbed by J_{20}-term traces a circle with a radius $(3/2) \cdot J_2 \cdot (a_e/a)^2$ in a (ξ, ζ) plane synchronizing with the satellite motion.

For lunar gravity:

$$\begin{pmatrix} \Delta\xi_\leftmoon \\ \Delta\eta_\leftmoon \end{pmatrix} = \begin{pmatrix} \cos\Omega & -\sin\Omega \\ \sin\Omega & \cos\Omega \end{pmatrix} \begin{pmatrix} \Delta\xi'_\leftmoon \\ \Delta\eta'_\leftmoon \end{pmatrix} \qquad (2)$$

$$\begin{pmatrix} \Delta\xi'_\leftmoon \\ \Delta\eta'_\leftmoon \end{pmatrix} = \frac{n}{n - n_\leftmoon} \cdot \frac{m_\leftmoon}{m_\oplus} \left(\frac{a}{r_\leftmoon}\right)^3$$

$$\Bigg[\Bigg\{1 - \frac{2}{3}(A^2 + B^2)\Bigg\} \begin{pmatrix} \cos(\omega + M) \\ \sin(\omega + M) \end{pmatrix}$$

$$+ \frac{A^2 - B^2}{4} \begin{pmatrix} \cos 3(\omega + M) + 9\cos(\omega + M) \\ \sin 3(\omega + M) + 9\sin(\omega + M) \end{pmatrix}$$

$$+ \frac{AB}{2} \begin{pmatrix} \sin 3(\omega + M) + 9\sin(\omega + M) \\ -\cos 3(\omega + M) + 9\cos(\omega + M) \end{pmatrix}$$

$$+ \frac{3}{8} \frac{a}{r_\leftmoon} \Bigg[\Bigg\{1 - \frac{5}{4}(A^2 + B^2)\Bigg\} \begin{pmatrix} A\cos 2(\omega + M) + B\sin 2(\omega + M) \\ A\sin 2(\omega + M) - B\cos 2(\omega + M) \end{pmatrix}$$

$$+ \frac{5}{4} A(A^2 - 3B^2) \begin{pmatrix} 3\cos 2(\omega+M) + \frac{1}{2}\cos 4(\omega+M) \\ -3\sin 2(\omega+M) + \frac{1}{2}\sin 4(\omega+M) \end{pmatrix}$$

$$+ \frac{5}{4} B(3A^2 - B^2) \begin{pmatrix} 3\sin 2(\omega+M) + \frac{1}{2}\sin 4(\omega+M) \\ 3\cos 2(\omega+M) - \frac{1}{2}\cos 4(\omega+M) \end{pmatrix}\Bigg]\Bigg] \qquad (3)$$

where n is the mean motion of the satellite, $n_\leftmoon$ the mean motion of the moon, $m_\oplus$ the mass of the earth, $r_\leftmoon$ the distance between earth and moon. A and B are:

$$A = \cos\delta_\leftmoon \cos(\Omega - \alpha_\leftmoon)$$

$$B = -\cos\delta_\leftmoon \cos i \sin(\Omega - \alpha_\leftmoon) + \sin\delta_\leftmoon \sin i$$

where $(\alpha_\leftmoon, \delta_\leftmoon)$ are the right ascension and the declination of the moon.
Subscript $\leftmoon$ represents a value for the moon and $\oplus$ represents a value for the earth.

Eq.(3) indicates that the e-vector perturbed by lunar gravity nearly traces a diamond shape in (ξ, η) plane. The variation of e-vector due to solar gravity also be given by the expressions of the same form as the equations (2) and (3).

2.2 Long-period and secular perturbations

In order to determine an optimum station-keeping strategy, it is necessary to know the changes in the mean elements caused by long-period and secular perturbations. Perturbations of the semi-major axis and the drift-rate, the inclination vector, and the eccentricity vector during the interval between maneuvers must be taken into account.

2.2.1 Semi-major axis and drift-rate. The long-period perturbations of the semi-major axis are caused by mainly non-zonal terms of earth's triaxiality. This in turn causes a long-period acceleration of the mean subsatellite longitude. The acceleration of the mean subsatellite longitude is about 1.5×10^{-3} deg·day^{-2} westward at 135° east longitude.

On the other hand, the oblateness of the earth and the luni-solar gravity generate the secular perturbations of Ω, ω, and n. The former causes the increase of about 2Km in the geosynchronous radius and the latter causes the decrease of about 0.5Km in it.

2.2.2 Inclination vector. J_{20}-term and luni-solar gravity cause the drift of the inclination vector. The mean value of the drift motion of the inclination is about 0.8° per year. By choosing the initial ascending node close to 270°, the inclination decreases first to zero, and then increases. This property is used for determining an optimum north-south station-keeping strategy. The motion of the i-vector due to these perturbations is given by:

$$\kappa = \gamma \textcircled{2} \begin{bmatrix} 1 + 0.00016t\,\textcircled{\frac{1}{2}} - 0.00434\,\textcircled{N} + 0.00419\,\textcircled{N}^{-1} + 0.00003\,\textcircled{N}^{2} - 0.00002\,\textcircled{N}^{-2} \\ +0.00004\,(-\textcircled{\omega_\odot}^{-1}\textcircled{\lambda_\odot} + \textcircled{\omega_\odot}\textcircled{\lambda_\odot}^{-1}) - 0.00001\,\textcircled{N}^{-1}\textcircled{\lambda_\odot}^{2} \\ -0.00011\,\textcircled{\lambda_\odot}^{2} + 0.00012\,\textcircled{\lambda_\odot}^{-2} \\ +0.00002\,(-\textcircled{\omega_\zeta}^{-1}\textcircled{\lambda_\zeta} + \textcircled{\omega_\zeta}\textcircled{\lambda_\zeta}^{-1}) + 0.00001\,(-\textcircled{N}^{-1}\textcircled{\lambda_\zeta}^{2} + \textcircled{N}\textcircled{\lambda_\zeta}^{-2}) \\ +0.00002\,(-\textcircled{\lambda_\zeta}^{2} + \textcircled{\lambda_\zeta}^{-2}) \end{bmatrix}$$

$$+\gamma \textcircled{2}^{-1} \begin{bmatrix} 0.01445 - 0.01020\,\textcircled{N} - 0.00008\,\textcircled{N}^{-1} - 0.00022\,\textcircled{N}^{2} \\ -0.00001\,\textcircled{\omega_\odot}\textcircled{\lambda_\odot} + 0.00092\,\textcircled{\lambda_\odot}^{2} + 0.00004\,\textcircled{\omega_\odot}^{-1}\textcircled{\lambda_\odot}^{3} \\ -0.00001\,\textcircled{\omega_\zeta}\textcircled{\lambda_\zeta} + 0.00015\,\textcircled{\lambda_\zeta}^{2} + 0.00002\,\textcircled{\omega_\zeta}^{-1}\textcircled{\lambda_\zeta}^{3} \end{bmatrix}$$

$$+0.132150 - 0.010662\,\textcircled{N} - 0.000359\,\textcircled{N}^{-1} + 0.000089\,\textcircled{N}^{2} + 0.000001\,\textcircled{N}^{-2}$$
$$+0.000013\,\textcircled{\omega_\odot}^{-1}\textcircled{\lambda_\odot} - 0.000014\,\textcircled{\omega_\odot}\textcircled{\lambda_\odot}^{-1} + 0.000005\,\textcircled{\omega_\odot}\textcircled{\lambda_\odot}$$
$$+(-0.000279 - 0.000010\,\textcircled{N}^{-1})\textcircled{\lambda_\odot}^{2} + 0.000001\,\textcircled{N}\,(\textcircled{\lambda_\odot}^{2} - \textcircled{\lambda_\odot}^{-2})$$
$$-0.000010\,\textcircled{\omega_\odot}^{-1}\textcircled{\lambda_\odot}^{3} - 0.000001\,\textcircled{\omega_\odot}\textcircled{\lambda_\odot}^{-3}$$
$$+(0.000007 + 0.000002\,\textcircled{N})(\textcircled{\omega_\zeta}^{-1}\textcircled{\lambda_\zeta} - \textcircled{\omega_\zeta}\textcircled{\lambda_\zeta}^{-1}) + (0.000002 + 0.000001\,\textcircled{N}^{-1})\textcircled{\omega_\zeta}\textcircled{\lambda_\zeta}$$
$$-0.000016\,\textcircled{N}^{-1}\textcircled{\lambda_\zeta}^{2} - 0.000001\,\textcircled{N}\,\textcircled{\lambda_\zeta}^{-2} + (-0.000046 + 0.000001\,\textcircled{N})\textcircled{\lambda_\zeta}^{2}$$
$$+(-0.000006 - 0.000002\,\textcircled{N}^{-1})\textcircled{\omega_\zeta}^{-1}\textcircled{\lambda_\zeta}^{3} - 0.000001\,\textcircled{\omega_\zeta}^{-2}\textcircled{\lambda_\zeta}^{4}$$

where

$$\kappa = P + jq$$

$$\textcircled{\theta} = e^{j\theta}$$

$$\dot{\beta} = \beta_0 + \dot{\beta}t$$

$$\dot{\beta} = -3.19459 \times 10^{-4} \text{ (rad/day)}$$

$$\lambda_{\odot/\mathfrak{k}} = \Omega_{\odot/\mathfrak{k}} + \omega_{\odot/\mathfrak{k}} + M_{\odot/\mathfrak{k}}$$

$$\bar{\omega}_{\odot/\mathfrak{k}} = \Omega_{\odot/\mathfrak{k}} + \omega_{\odot/\mathfrak{k}}$$

N = longitude of the ascending node of the moon referred to the ecliptic plane.

Subscript $\odot$ represents a value for the sun. And, γ and β_0 are the constants determined from the initial conditions.

2.2.3 Eccentricity vector. Solar radiation pressure and lunar gravity generate variations of eccentricity vector with the period of 1 year and 1 month respectively. The motion of e-vector due to these long-period perturbing force is given by the following equations.

For solar radiation pressure:

$$\varepsilon_c = \varepsilon_{c0} + \Delta\varepsilon_c$$

$$\Delta\varepsilon_c = F\left(0.000096\left(\bar{\omega}_\odot\right) - 0.000009\left(\bar{\omega}_\odot\right)^{-1} - 0.000001\left(\bar{\omega}_\odot\right)^{-1}\left(N\right) + \left(\bar{\omega}_\odot\right)\left(N\right)^{-1}\right)$$
$$+0.000108\left(\lambda_\odot\right) - 0.000005\left(\lambda_\odot\right)^{-1} + 0.000001\left(\bar{\omega}_\odot\right)^{-1}\left(\lambda_\odot\right)^2\Big) \qquad (5)$$

where $\varepsilon_c = \xi + \zeta$

ε_{c0} = initial value of ε_c

$$F = C_R \frac{A}{W} P \frac{5 \times 10^6}{n^2 a}$$

where C_R is the surface reflectivity of a satellite, A the cross sectional area of a satellite, W satellite weight, and P the solar constant.
Let $(x_\odot, y_\odot)$ is the (x,y) component of the unit sun vector in the equatorial coordinate system, then, $d\xi/dt$ and $d\eta/dt$ are:

$$\begin{pmatrix} \frac{d\xi}{dt} \\ \frac{d\eta}{dt} \end{pmatrix} = \frac{3C_R AP}{2Wna} \begin{pmatrix} -y_\odot \\ x_\odot \end{pmatrix} \qquad (6)$$

Eq.(6) indicates that the e-vector perturbed by solar radiation pressure traces a circle in the (ξ, η) plane synchronizing with the sun motion as shown in Fig. 1. The radius of the circle is given by

$$R_{sp} = \frac{3C_R AP}{2nan_\odot w} \qquad (7)$$

For lunar gravity:

$$\varepsilon_c = \kappa\left(\alpha\right)\left(1 + 0.016t\left(\frac{\pi}{2}\right) + 0.005\left(N\right) - 0.004\left(N\right)^{-1}\right)$$
$$+\kappa\left(\alpha\right)^{-1}\left[-0.069 + 0.001t\left(\frac{\pi}{2}\right) - 0.008\left(N\right) + 0.005\left(\lambda_\odot\right)^2 + 0.001\left(\lambda_\zeta\right)^2\right)$$
$$+\left(-0.000205 + 0.000068\left(N\right) + 0.000019\left(N\right)^{-1} + 0.000006\left(N\right)^2\right)\left(\bar{\omega}_\zeta\right)$$
$$+\left(0.000058 + 0.000016\left(N\right) - 0.000006\left(N\right)^{-1} + 0.000001\left(N\right)^2\right)\left(\bar{\omega}_\zeta\right)^{-1}$$
$$-0.000001\left(\bar{\omega}_\zeta\right)^{-1}\left(\lambda_\odot\right)^2$$
$$-0.000027\left(\lambda_\zeta\right) + 0.000010\left(\lambda_\zeta\right)^{-1} + 0.000004\left(\left(N\right)\left(\lambda_\zeta\right) + \left(N\right)^{-1}\left(\lambda_\zeta\right) + \left(N\right)\left(\lambda_\zeta\right)^{-1}\right)$$
$$-0.000002\left(\bar{\omega}_\zeta\right)^{-1}\left(\lambda_\zeta\right)^2 + 0.000001\left(\bar{\omega}_\zeta\right)\left(\lambda_\zeta\right)^{-2}$$
$$+\left(-0.000003 - 0.000001\left(N\right)^{-1}\right)\left(\lambda_\zeta\right)^3 - 0.000001\left(\bar{\omega}_\zeta\right)^{-1}\left(\lambda_\zeta\right)^4 \qquad (8)$$

where

$$\alpha = \alpha_0 + \alpha t$$

$$\alpha = 3.1600 \times 10^{-4} \text{ (rad/day)}$$

K and α_0 are the constants determined from the initial conditions.

The motion of e-vector due to lunar gravity is nearly synchronizing with the moon motion as shown in Fig. 2.

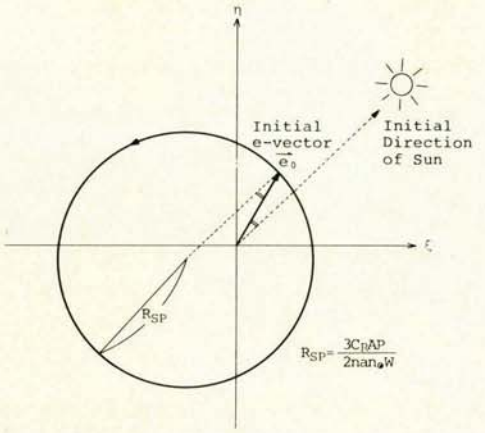

Figure 1. Motion of e-vector due to Solar Radiation Pressure

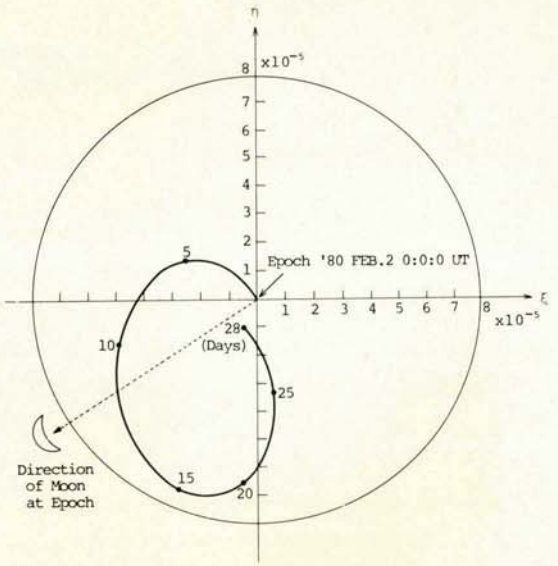

Figure 2. Motion of e-vector due to Lunar Gravity

3. ORBIT CHANGE BY IMPULSIVE VELOCITY CORRECTION

In order to consider the effect of an impulsive velocity increment on the elements of near geostationary orbit, the following matrix is used:

$$\frac{\partial\begin{pmatrix} a \\ \Sigma \\ p \\ q \\ \xi \\ \eta \end{pmatrix}}{\partial\begin{pmatrix} \dot{x} \\ \dot{y} \\ \dot{z} \end{pmatrix}} = \begin{pmatrix} -\frac{2}{n}\sin\Sigma & \frac{2}{n}\cos\Sigma & 0 \\ -\frac{2}{na}\cos\Sigma & -\frac{2}{na}\sin\Sigma & 0 \\ 0 & 0 & \frac{1}{na}\cos\Sigma \\ 0 & 0 & \frac{1}{na}\sin\Sigma \\ -\frac{1}{2na}\sin 2\Sigma & \frac{1}{2na}(\cos 2\Sigma + 3) & 0 \\ \frac{1}{2na}(\cos 2\Sigma - 3) & \frac{1}{2na}\sin 2\Sigma & 0 \end{pmatrix} \tag{9}$$

where $(\dot{x}, \dot{y}, \dot{z})$ is the velocity vector in the equatorial coordinate system.

From the Eq.(9), it is possible to obtain the equations for impulsive changes in the components of the vector elements. The components of an impulsive velocity increment ΔV $(\Delta\dot{x}, \Delta\dot{y}, \Delta\dot{z})$ are expressed as follows:

$$\begin{aligned} \Delta\dot{x} &= \Delta V \cos\delta \cos\alpha = \Delta V_{IN} \cos\alpha \\ \Delta\dot{y} &= \Delta V \cos\delta \sin\alpha = \Delta V_{IN} \sin\alpha \\ \Delta\dot{z} &= \Delta V \sin\delta = \Delta V_N \end{aligned}$$

where ΔV is the magnitude of $\overrightarrow{\Delta V}$, (α, δ) the right ascension and the declination of $\overrightarrow{\Delta V}$ direction, ΔV_{IN} the in-plane component of $\overrightarrow{\Delta V}$, and ΔV_N is the component normal to a orbital plane. Then, the changes of the elements due to $\overrightarrow{\Delta V}$ is given by:

$$\begin{pmatrix} \Delta a \\ \Delta\Sigma \\ \Delta p \\ \Delta q \\ \Delta\xi \\ \Delta\eta \end{pmatrix} = \frac{\partial\begin{pmatrix} a \\ \Sigma \\ p \\ q \\ \xi \\ \eta \end{pmatrix}}{\partial\begin{pmatrix} \dot{x} \\ \dot{y} \\ \dot{z} \end{pmatrix}} \begin{pmatrix} \Delta\dot{x} \\ \Delta\dot{y} \\ \Delta\dot{z} \end{pmatrix} \tag{10}$$

3.1 Semi-major axis and mean right ascension

The changes in the semi-major axis and the mean right ascension due to impulsive velocity increment are given by:

$$\begin{aligned} \begin{pmatrix} \Delta a \\ \Delta\Sigma \end{pmatrix} &= \frac{\partial\begin{pmatrix} a \\ \Sigma \end{pmatrix}}{\partial\begin{pmatrix} \dot{x} \\ \dot{y} \end{pmatrix}} \begin{pmatrix} \Delta\dot{x} \\ \Delta\dot{y} \end{pmatrix} \\ &= -\frac{2\Delta V_{IN}}{V_0} \begin{pmatrix} a\sin\Sigma & -a\cos\Sigma \\ \cos\Sigma & \sin\Sigma \end{pmatrix} \begin{pmatrix} \cos\alpha \\ \sin\alpha \end{pmatrix} \\ &= -\frac{2\Delta V_{IN}}{V_0} \begin{pmatrix} a\sin(\Sigma - \alpha) \\ \cos(\Sigma - \alpha) \end{pmatrix} \end{aligned} \tag{11}$$

where V_0 is the initial orbital velocity.
From Eq.(11), the drift-rate change $\Delta\dot{\lambda}$ is expressed by:

$$\begin{aligned} \Delta\dot{\lambda} &= -\frac{3}{2}\frac{\Delta a}{a} n \\ &= \frac{3\Delta V_{IN} n}{V} \sin(\Sigma - \alpha) \end{aligned} \tag{12}$$

3.2 Inclination vector

The change in the inclination vector is given by:

$$\begin{pmatrix} \Delta p \\ \Delta q \end{pmatrix} = \frac{\partial\begin{pmatrix} p \\ q \end{pmatrix}}{\partial\dot{z}} \Delta\dot{z} = \frac{\Delta V_N}{V_0} \begin{pmatrix} \cos\Sigma \\ \sin\Sigma \end{pmatrix} \tag{13}$$

This change is illustrated in Fig. 3.

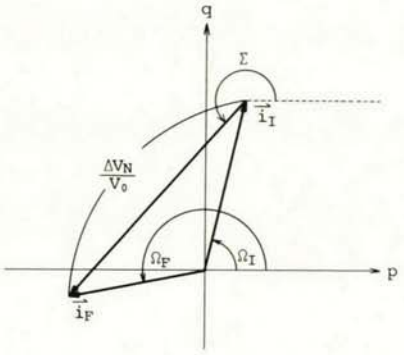

Figure 3. Change in i-vector due to Impulsive Velocity Correction

3.3 Eccentricity vector

The change in the eccentricity vector is given by:

$$\begin{aligned} \begin{pmatrix} \Delta\xi \\ \Delta\eta \end{pmatrix} &= \frac{\partial\begin{pmatrix} \xi \\ \eta \end{pmatrix}}{\partial\begin{pmatrix} \dot{x} \\ \dot{y} \end{pmatrix}} \begin{pmatrix} \Delta\dot{x} \\ \Delta\dot{y} \end{pmatrix} = \frac{\Delta V_{IN}}{2V_0} \begin{pmatrix} -\sin 2\Sigma & \cos 2\Sigma + 3 \\ \cos\Sigma - 3 & \sin 2\Sigma \end{pmatrix} \begin{pmatrix} \cos\alpha \\ \sin\alpha \end{pmatrix} \\ &= \frac{\Delta V_{IN}}{V_0} \begin{pmatrix} \cos\Sigma & -\sin\Sigma \\ \sin\Sigma & \cos\Sigma \end{pmatrix} \begin{pmatrix} 2\sin(\alpha - \Sigma) \\ -\cos(\alpha - \Sigma) \end{pmatrix} \\ &= \frac{\Delta V_{IN}}{2V_0} \begin{pmatrix} \sin(\alpha - 2\Sigma) \\ \cos(\alpha - 2\Sigma) \end{pmatrix} + \frac{3\Delta V_{IN}}{2V_0} \begin{pmatrix} \sin\alpha \\ -\cos\alpha \end{pmatrix} \end{aligned} \tag{14}$$

when $\alpha = \Sigma + 90°$, $(\Delta\xi, \Delta\eta)$ is illustrated in Fig. 4.

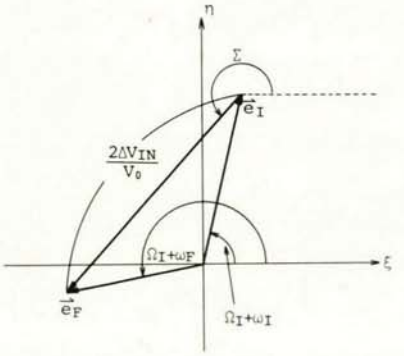

Figure 4. Change in e-vector due to Impulsive Velocity Correction ($\alpha = \Sigma + 90°$)

4. E-W STATION KEEPING STRATEGY

The objective of the east-west station-keeping is to maintain a satellite within a tolerable range around a target geostationary longitude. The variation of the sub-satellite longitude of a geostationary satellite is caused mainly by the following two effects:

- A long-period perturbation of the semi-major axis due to J_{22} tesseral term,
- A long-period perturbation of the eccentricity due to solar radiation pressure. The satellite will have a daily oscillation in the subsatellite longitude with amplitude $|2e|$.

In NASDA, the east-west station-keeping maneuver operation has been carried out based on "Sun-synchronized Method" which is described in the sequel.

4.1 Sun-synchronized Method

The east-west station-keeping maneuver based on Sun-synchronized method provides both the required drift-rate and the eccentricity vector correction by one tangential velocity impulse. The motion of the mean subsatellite longitude and the drift-rate will trace a parabola in the $(\lambda,\dot{\lambda})$ plane such as shown in Fig. 5.

Assume that it is required to maintain a satellite around 135°E. The maneuver cycle begins at point A with the satellite positioned at the western edge of the band. The satellite initially drifts eastward. At B, the drift stops and changes the direction westward. When point C is reached, the station-keeping maneuver is made to aim at A by a tangential velocity impulse. This tangential velocity impulse also can be used for the correction of the e-vector.

The eccentricity vector moves, as mentioned in 2.2.3, on the circle synchronized with sun motion with a radius Rsp. Using this property, this radius can be reduced to an effective radius Rt by applying the tangential velocity impulse at an appropriate time. If θ is assumed to be small, Rt is given by:

$$Rt \fallingdotseq \frac{|\Delta e_p - \Delta e_{EW}|}{2\cdot\tan(\theta/2)} \qquad (15)$$

where Δe_p is the change in eccentricity during the interval T between maneuvers, and Δe_{EW} is the change caused by a maneuver, and θ is the change in right ascension of sun's direction during T. The correction sequence and its effect on eccentricity vector according to the sun-synchronized method are illustrated in Fig. 6 and Fig. 7. The maneuver cycle begins at point A. The eccentricity vector drifts on the circle with the radius Rsp without corrections during the interval of length T. At point B, a tangential velocity correction ΔV_{EW} is applied at 18 o'clock of local time. Then follows the next cycle.

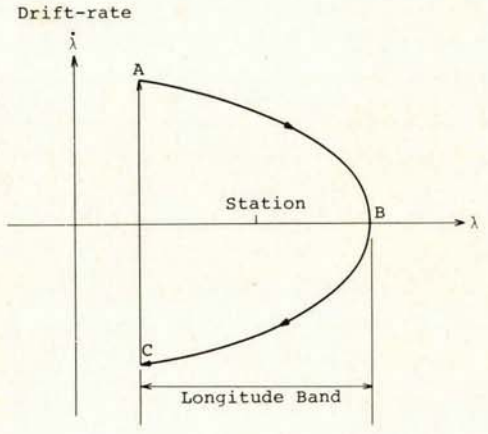

Figure 5. Motion of Sub-satellite Longitude and Drift-rate

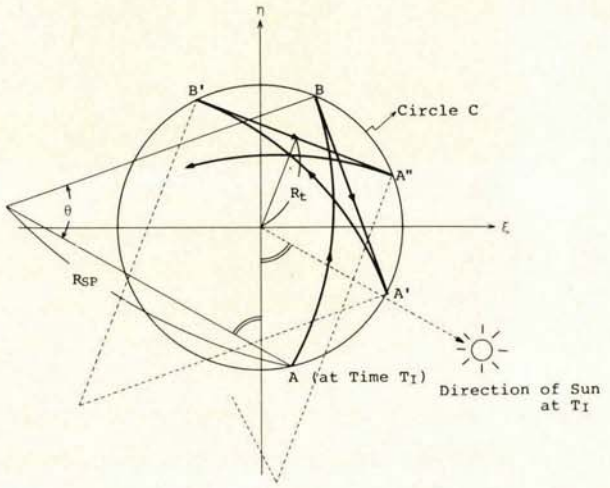

Figure 6. Motion of e-vector in Correction Cycle: $|\Delta e_P| > |\Delta e_{EW}|$

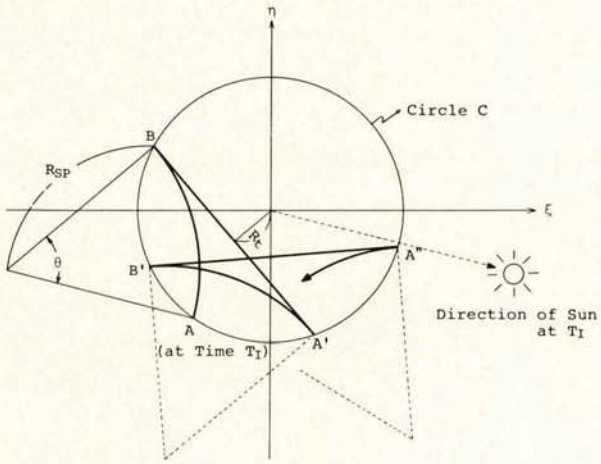

Figure 7. Motion of e-vector in Correction Cycle: $|\Delta e_{EW}| > |\Delta e_P|$

As observed from Fig. 6 and 7, when this method is applied to the eccentricity keeping, the initial eccentricity vector must be located at an appropriate point on the circle C relative to sun's direction. In the east-west station-keeping maneuver operations based upon Sun-synchronized method, every maneuver can be operated at almost same hour, at about 18 o'clock of local time.
Unless the initial e-vector is located at a suitable point for Sun-synchronized method, several maneuvers in the beginning of east-west station-keeping operations have to be carried out in order to acquire such a suitable point as point A in Fig.

6 and 7. In this interval, the time of the maneuver operation varies from maneuver to maneuver.

4.2 Operational longitude band

In order to maintain a satellite within a dead band in longitude which is determined from satellite mission requirements, an operational band has to be reduced from the dead band. The width of operational band depends upon the accuracies in orbit determination/prediction and in the APS (auxiliary propulsion system) thrusting error, and the magnitude of eccentricity. This is determined as shown in Fig. 8. In Fig. 8:

$\Delta\lambda_D$ = width of a dead band

$\Delta\lambda_{OP}$= width of an operational band

λ_T = target stationary longitude

λ_W = western edge of the dead band (= $\lambda_T - \Delta\lambda_D/2$)

λ_E = eastern edge of the dead band (= $\lambda_T + \Delta\lambda_D/2$)

$\Delta\lambda_e$ = daily oscillation in longitude due to eccentricity (= $|2e|$)

$\Delta\lambda_W$ = drift-rate at western edge

$\Delta\lambda_E$ = error in longitude at eastern edge resulting from orbit prediction and APS thrusting.

We assume that daily oscillation in longitude due to inclination can be neglected.
Thus, one cycle for the east-west station-keeping maneuver strategy consists of:

i) sub-satellite longitude initially at $\lambda_W + \Delta\lambda e + \Delta\lambda_W$

ii) drift phase from $\lambda_W + \Delta\lambda e + \Delta\lambda_W$ to $\lambda_E - \Delta\lambda e - \Delta\lambda_E$

iii) drift phase from $\lambda_E - \Delta\lambda e - \Delta\lambda_E$ to $\lambda_W + \Delta\lambda e + \Delta\lambda_W$

iv) correction maneuver at $\lambda_W + \Delta\lambda e + \Delta\lambda_W$ which reverses the drift-rate and corrects e-vector simultaneously.

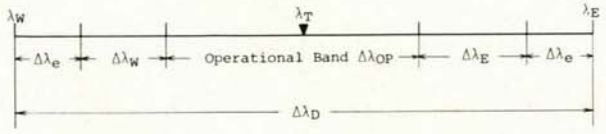

Figure 8. Operational Longitude Band for E/W Station Keeping

5. MANEUVER EVALUATION

When maneuver commands computed on the ground using the thruster data tables are executed in the space environment, the resulting satellite orbital parameters will usually differ from the expected values. The objective of maneuver evaluation is to determine correction coefficients to be applied on the thruster data tables in order to simulate the actual flight performance of each thruster. The results of an executed command is, of course, obtained by orbit determination.

For the east-west station-keeping maneuver which is operated using a thruster in the pulsed firing mode, impulsive velocity increment (ΔV_{IN}) and the right ascension of ΔV vector (α) are evaluated. On the other hand, for the north-south station-keeping maneuver which is operated using a thruster in the continuous firing mode, ΔV_N and the maneuver centroid time (tm), at which ΔV_N assumed to be applied instantaneously, are evaluated. The method of maneuver evaluation using semi-major axis, e-vector, and i-vector is described in the sequel.

5.1 Evaluation by semi-major axis

The subscript I represents an initial value prior to the maneuver, the subscript R represents an actual value obtained by orbit determination performed after the maneuver, and the subscript E represents an expected value computed by a command generation program.
An estimated ratio of the actual value of ΔV_{IN} to the expected value is given by:

$$\zeta_a = \frac{a_R - a_I}{a_E - a_I} \tag{16}$$

ζ_a is used as an efficiency coefficient to be applied on the cumulative impulse data table for the east-west station-keeping maneuver.

5.2 Evaluation by i-vector

An efficiency coefficient to be applied on the thrust data table for the north-south station-keeping maneuver is given by:

$$\zeta_i = \frac{|\overrightarrow{\Delta i_R}|}{|\overrightarrow{\Delta i_E}|} = \frac{|\vec{i}_R - \vec{i}_I|}{|\vec{i}_E - \vec{i}_I|} \tag{17}$$

The angle from $\overrightarrow{\Delta i_E}$ to $\overrightarrow{\Delta i_R}$ corresponds to the error in the maneuver centroid time.

5.3 Evaluation by e-vector

Assume that the in-plane velocity increment $\overrightarrow{\Delta V_{IN}} = (\Delta V_R, \Delta V_T)$, where ΔV_R is the radial component in the orbital plane, positive outward, ΔV_T is the tangential component, positive in the direction of motion. In Eq.(14), ΔV_R and ΔV_T correspond to $\alpha = \Sigma$ and $\alpha = \Sigma + 90°$ respectively. Then the change in e-vector may be expressed in terms of ΔV_T and ΔV_R by:

$$\begin{pmatrix}\Delta\xi\\ \Delta\eta\end{pmatrix} = \frac{2\Delta V_T}{V_0}\begin{pmatrix}\cos\Sigma\\ \sin\Sigma\end{pmatrix} + \frac{\Delta V_R}{V_0}\begin{pmatrix}\sin\Sigma\\ -\cos\Sigma\end{pmatrix} \tag{18}$$

This is illustrated in Fig. 9.
Eq.(18) shows that an eccentricity vector can be changed by either a tangential velocity impulse or a radial velocity impulse. Using this property, it is possible to evaluate both an impulsive velocity increment and it's directional error (i.e., the error in right ascension of ΔV_{IN}) for the east-west station-keeping maneuver.
From Eq.(14),

$$\textcircled{-\Sigma}\begin{pmatrix}\Delta\xi\\ \Delta\eta\end{pmatrix} = \frac{\Delta V_{IN}}{V_0}\begin{pmatrix}2\sin(\alpha-\Sigma)\\ -\cos(\alpha-\Sigma)\end{pmatrix} \tag{19}$$

where

$$\textcircled{-\Sigma} = \begin{pmatrix}\cos\Sigma & -\sin\Sigma\\ \sin\Sigma & \cos\Sigma\end{pmatrix}$$

Let

$$\ominus(\Sigma)\begin{pmatrix}\Delta\xi\\ \Delta\eta\end{pmatrix}=\begin{pmatrix}\Delta\xi'\\ \Delta\eta'\end{pmatrix}$$

and

$$A=\sqrt{(\Delta\xi'/2)^2+(\Delta\eta')^2}$$

Then, the efficiency coefficient for an in-plane impulsive velocity increment maneuver is given by:

$$\zeta_e=\frac{A_R}{A_E} \tag{20}$$

ζ_e is also used to calibrate the cumulative impulse data table for the east-west station-keeping maneuver, as well as ζ_a.
The right ascension of ΔV_{IN} is given by:

$$\alpha=\tan^{-1}\left(\frac{\Delta\xi'}{-2\Delta\eta'}\right)+\Sigma \tag{21}$$

Then the directional error in ΔV_{IN} is given by:

$$\Delta\alpha=\alpha_R-\alpha_E \tag{22}$$

$\Delta\alpha$ is used to calculate the efficiency coefficient to be applied on the thrust centroid data table for the east-west station-keeping maneuver. The thrust centroid is defined as the time measured from the point at which the thruster valve is opened to the central point of the pulse.

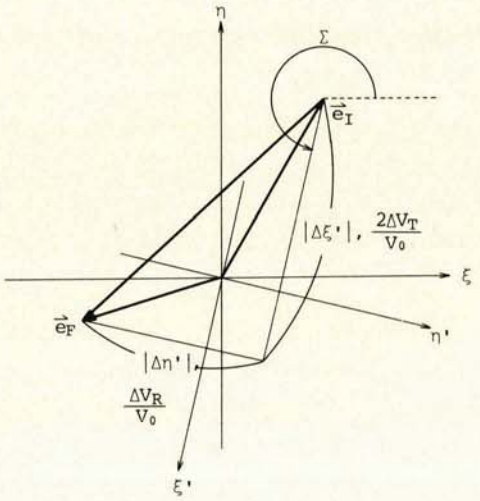

Figure 9. Change in e-vector due to Impulsive Velocity Correction

6. RESULTS ON CS

CS was launched from Eastern Test Range, Florida, U. S. A. by a Delta 2914 on December 24, 1977. Ten days after the launch, it was placed on-station at 135° east longitude. Since then, based upon Sun-synchronized method, many east-west station-keeping maneuvers have been carried out. During the required mission duration of CS, it is necessary to maintain it's longitude within ±0.1° from 135° east longitude station.

Fig. 10 shows the operational band for CS E-W station-keeping maneuver strategy.

Fig. 11 and 12 show CS E-W station-keeping maneuver history. These maneuvers have been carried out every 21 days. The velocity increment for each maneuver was about 0.1 m/sec consuming about 0.002 Kg hydrazine.

Fig. 11 shows a history of subsatellite longitude and drift-rate from April 1979 to March 1980. In this figure, broken lines which correspond to the maneuvers tend to lean towards the left.
It is supposed that these leanings are induced by the error in semi-major axis resulting from orbit determination. These correspond to about 50 meters of the error in semi-major axis.

Fig. 12 shows a history of the mean eccentricity vector in about 1 year from April 1979 to March 1980.

Fig. 13 is a graph showing efficiency coefficients for CS's radial thrusters vs. pulse number.

And, Fig. 14 is a graph showing the directional errors of the maneuvers vs. pulse number.

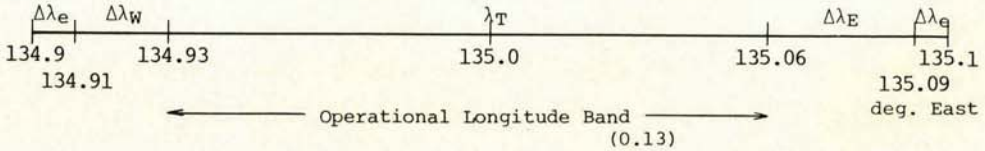

Magnitude of $\Delta\lambda_e$, $\Delta\lambda_E$, and $\Delta\lambda_E$ correspond to:

maximum eccentricity ; 1×10^{-4}
orbit determination error ; 50 m in semi-major axis
maneuver error ; 5%

Figure 10. CS Operational Longitude for E/W Station-Keeping

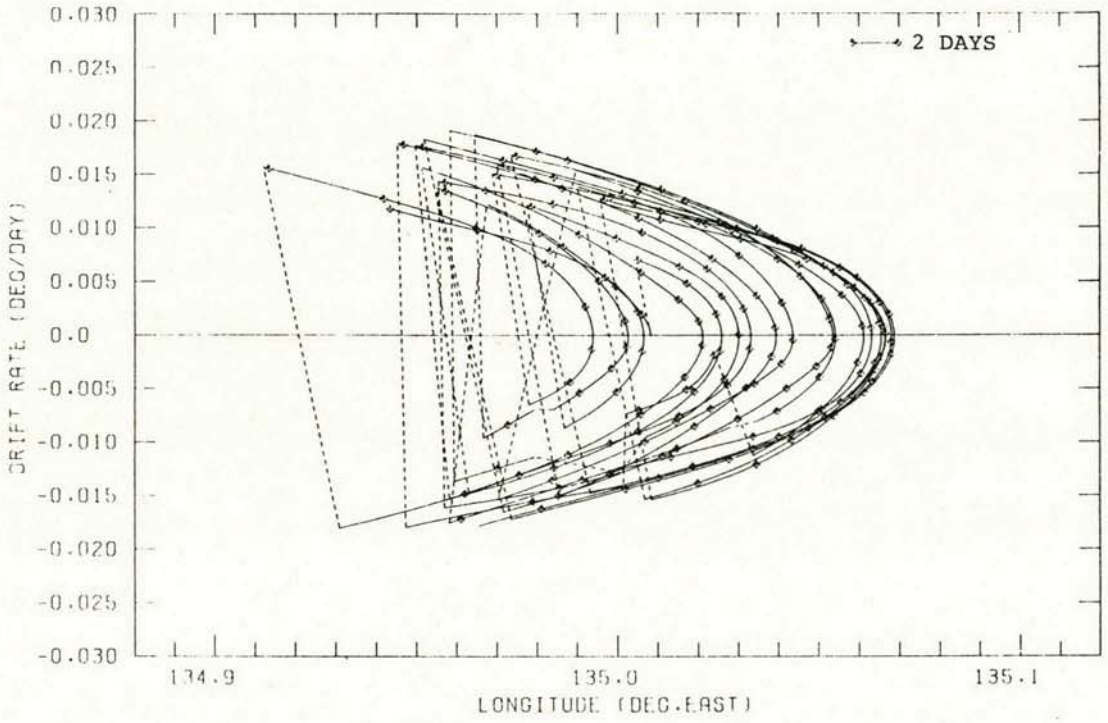

Figure 11. CS Sub-satellite and Drift Rate History

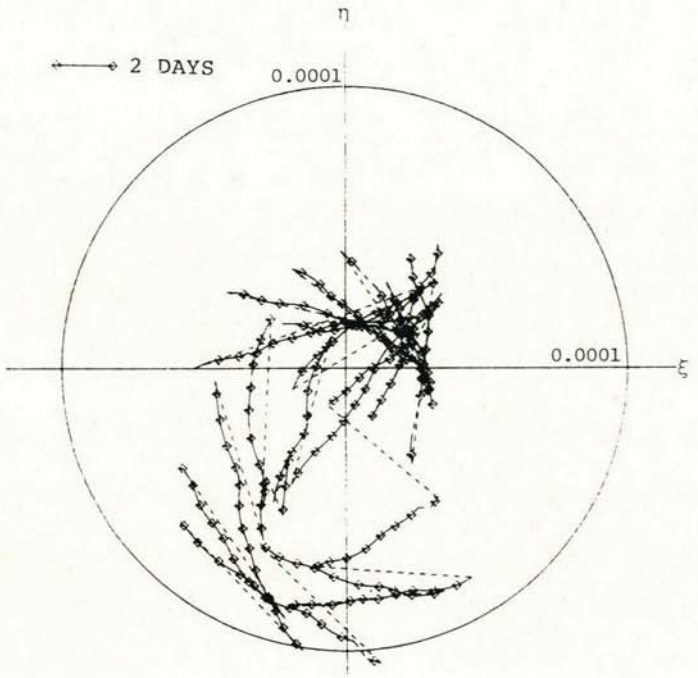

Figure 12. CS Mean Eccentricity Vector History

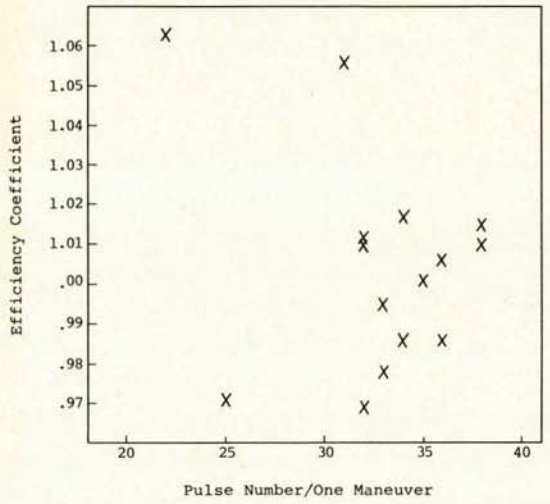

Figure 13. Efficiency Coefficient vs. Pulse Number for CS Radial Thruster

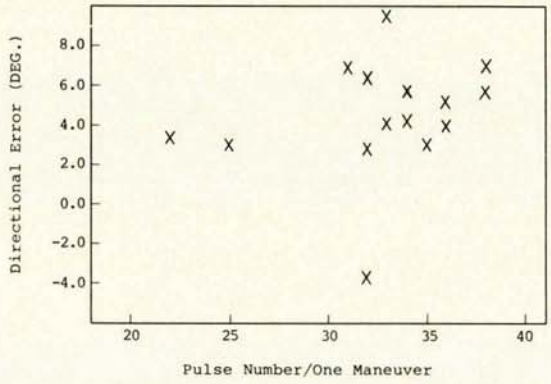

Figure 14. Directional Error vs. Pulse Number for CS Radial Thruster

7. CONCLUSION

This method has been applied also to the Engineering Test Satellite II (ETS-II), the Geostationary Meteorological Satellite (GMS) and the Medium-Scale Broadcasting Satellite for Experimental Purposes (BSE), and all the results have been wholly successful. These results confirm the validity of NASDA's east-west station-keeping maneuver strategy and maneuver evaluation technique.

8. ACKNOWLEDGEMENTS

The authors wish to acknowledge the many useful discussions with Dr. T. Takenouchi, Mr. M. Hirota, and Mr. S. Mori of NASDA. They also wish to thank Dr. T. Nishimura, International Institute for Advanced Study of Social Information Science, Japan, for his helpful suggestions.

9. REFERENCES

1. Hirota M et al 1978, Mathematical model description for maneuver programs (in Japanese), NASDA.

2. Balsam R E et al 1969, A simplified approach for correction of perturbations on a geostationary orbit, J Spacecraft, Vol 6, No. 7, July 1969, 805-811.

3. Tanaka A et al 1980, Station and Attitude Keeping of Japanese Communications Satellite for Experimental Purposes, XXXI Congress IAF'80, Tokyo 21-28 Sep 1980.